Title

Estimation of plane of maximum curvature for the patients with adolescent idiopathic scoliosis via a purpose-design computational method

Hui-Dong Wu, MSc[1,2,3]; Chen He, PhD[1,5]; Winnie Chiu-Wing Chu, MD[4]; Man-Sang Wong, PhD[1]

1 Department of Biomedical Engineering, The Hong Kong Polytechnic University, Hong Kong, China

2 Department of Rehabilitation Medicine, West China Hospital, Sichuan University, Chengdu, Sichuan, China

3 Institute for Disaster Management and Reconstruction, Sichuan University-Hong Kong Polytechnic University, Chengdu, Sichuan, China

4 Department of Imaging & Interventional Radiology, Faculty of Medicine, The Prince of Wales Hospital, The Chinese University of Hong Kong, Hong Kong, China

5 Institute of Rehabilitation Engineering and Technology, University of Shanghai for Science and Technology, Shanghai, China

Address correspondence and reprint requests to Man-Sang Wong, PhD, Department of Biomedical Engineering, The Hong Kong Polytechnic University, Hong Kong, China, Tel: (+852) 27667680; E-mail: m.s.wong@polyu.edu.hk.

Funding: No funding was received in support of this work.

Conflict of Interest: Author Hui-Dong Wu, Chen He, Winnie Chiu-Wing Chu, and Man-Sang Wong declare that they have no conflict of interest.

Acknowledgments: The CT Images were obtained from the Department of Imaging & Interventional Radiology, Chinese University of Hong Kong.

Abstract

Purpose The coronal Cobb angle is commonly used for assessing the adolescent idiopathic scoliosis (AIS), however, it may underestimate the severity of AIS while the PMC could be a promising descriptor for three-dimensional assessment of AIS. This study aimed to develop a computational method (CM) for estimating the plane of maximum curvature (PMC) based on the coronal and sagittal images of the spine, and to verify the results with computed tomography (CT).

Methods Twenty-eight thoracic and 24 lumbar curves from 30 subjects with AIS were analysed. For the CM, PMC was estimated via identifying the two corner points at the superior endplate of upper-end vertebra and the inferior endplate of lower-end vertebra in the coronal and sagittal CT images separately (eight corner points in total). For the CT, PMC was determined through rotating the spine images axially until the maximum Cobb angle was found. Intraclass correlation coefficient (ICC), Bland-Altman method, and linear regression analysis were used for the statistical analyses.

Results The high ICC values (intra->0.91; inter->0.84) suggested very good intra- and inter-rater reliability of the CM in PMC estimation. The high ICC values (>0.91) and assessment of Bland-Altman method demonstrated a good

agreement between PMC acquired using the CM and CT. The generated linear regression equations (R^2>0.69) could allow to estimate the PMC (originally measured through the CT) via the CM.
Conclusion The developed computational method could estimate reliable and valid PMC for the patients with AIS, and become feasible for three-dimensional assessment of AIS.

Keywords Plane of Maximum Curvature; Adolescent Idiopathic Scoliosis; Computed Tomography; Computational Method; Reliability and Validity

Level of evidence: 3

Introduction

Adolescent idiopathic scoliosis (AIS) is a complicated three-dimensional (3D) deformity of the spine characterized by lateral curve and vertebral rotation [1]. The Cobb angle measured from the coronal radiograph (coronal-Cobb) is considered as a gold standard for assessment of scoliosis [2], however, it may underestimate the severity of spinal curvature and may not fully reflect the curve types [3,4]. The plane of maximum curvature (PMC) has thereby been proposed. The PMC is defined as a vertical plane that positions between the sagittal and coronal planes and presents the maximum spinal curvature (Fig.1) [1]. Its parameters include the maximum Cobb angle in the PMC (PMC-Cobb) and orientation of PMC (PMC-orientation, the angle between the PMC and sagittal plane [5]). The PMC is promising in describing 3D features of the scoliotic spine [6], and increasing value in spine surgery [7]. It may have the potential to enhance the design of spinal orthosis in the determination of force applications.

The PMC could be estimated by rotating axially a plane where a spinal curve is projected onto until the maximum Cobb angle is found. However, 3D reconstruction of the scoliotic spine was required in this method [3,8,9]. On the other hand, the reliability and validity of the PMC estimation obtained from the 3D reconstructed spine have not been studied comprehensively. The computed tomography (CT), which is recognized as a useful tool of 3D assessment of scoliosis, could allow the PMC estimation. Nevertheless, this method is usually applied to either research purpose or severe cases, and seldom to mild or moderate cases because of high radiation exposure and time consumption. Therefore, this study aimed to propose and verify a user-friendly and less time-consuming computational method (CM) for estimating the PMC merely based on the coronal and sagittal images of the spine.

Methods

Subjects

In this retrospective study, the subjects were selected according to the criteria: (1) diagnosed with AIS; (2) age: 10-24; (3) coronal-Cobb: 10°-80°; (4) with CT images of the whole spine. Subjects who had prior surgical treatment or other diseases affecting the spinal profile were excluded.

A total of 30 subjects (28 females and 2 males with a mean age of 15.4±3.6) were selected from the database of a local hospital (no subjects were directly enrolled only for this study). All CT scans were taken in 2015-2017. Human subject ethical approval was granted from the authors' Institutional Review Board.

PMC estimation using the computational method (CM)

The CM was based on the global axis system (x, y, z) of the human body with the origin at the center of the superior endplate of the 1st sacral vertebra [10]. It assessed the spinal curve by calculating the angle formed by the intersection lines of a vertical plane and the superior endplate of the upper-end vertebra and inferior endplate of the lower-end vertebrae of a specific spinal curve. As shown in Fig. 2, to ensure the superior and inferior endplates of the end vertebrae being intersected by a single plane, this study assumed the two endplates to be on the planes that can be extended outward named $Plane_{superior\text{-}endplate}$ and $Plane_{inferior\text{-}endplate}$, respectively. The angle (β) formed by the intersection lines ($L_{vertical\text{-}superior}$ and $L_{vertical\text{-}inferior}$) was the Cobb angle of the spinal curve in that vertical plane. The orientation of that vertical plane was the angle between that vertical plane and the sagittal plane (θ). The maximum Cobb angle (β_{max}) was determined by calculating the Cobb angle in different vertical planes with an orientation interval of 1°. As shown in Fig.3: a) a rater identified eight corner points at the superior endplate of the upper-end vertebra and the inferior endplate of the lower-end vertebra in the sagittal and coronal CT images of the spine. Their 3D coordinates were used for Cobb angle (β) calculation, and the process was elaborated in Online Resource 1.

The orientation of the vertical plane (θ) was recorded as negative (-), and equal to 0°/-180° and -90°/-270° when overlapping with the sagittal and coronal planes, respectively. According to the quadrants that different curve types located at, the orientation (θ) ranged from (1) 0° to -90° and -270° to -359° for the right and left thoracic curves (RTs and LTs), respectively; (2) -90° to -180° and -180° to -270° for the right and left thoracolumbar/lumbar curves (RTLs/RLs and LTLs/LLs), respectively. With the pre-defined values of orientation (θ) at 0°, 1°, 2° … 358° and 359°, the Cobb angle in the vertical plane (under different pre-defined orientations) could be estimated in the Excel software (Microsoft Office 365, USA) according to the formula shown in Fig.2:d of the Online Resource 1, and the maximum Cobb angle (β_{max}) could be then determined. The plane showing the maximum Cobb angle (β_{max}) was considered as the PMC.

PMC estimation using the computed tomography (CT)

With all the CT images visualized three-dimensionally using an open-source image processing software named 3DSlicer (version 4.8.1, 3DSlicer Platform: www.slicer.org), a plane, where the spine was projected onto, was rotated 90° axially from the sagittal plane to the coronal plane with 5° increments. As shown in Fig.3: b) the Cobb angle in each rotated plane was measured using constrained and unconstrained Cobb methods which would be explained below. The maximum Cobb angle could be then identified, and the rotated plane presenting the maximum Cobb angle was recorded as the PMC.

The constrained Cobb method measures the Cobb angle in any other rotated images of the spine (different from the coronal image) but with the upper- and lower- end vertebrae constrained to the upper- and lower- end vertebrae pre-

selected from the coronal plane at the beginning of the measurement [8]; conversely, the unconstrained Cobb method measures the Cobb angle any other rotated images with the upper- and lower-end vertebrae determined from the instantly measured vertical plane. Due to the complexity of AIS, the constrained and unconstrained Cobb methods may not always provide the same PMC, and the latter may have a larger maximum Cobb angle in a certain vertical plane [8,11] and may better reflect the maximum spinal curvature. Thus, this study used both of them to verify the CM.

Data collection

Two raters with more than 3 years of experience in Cobb angle measurements participated in data collection. Based on the same set of the coronal and sagittal CT images of the spine, each rater used the CM to estimate the PMC 3 times (with a one-week interval to reduce possible recalling bias). One of the raters measured the PMC 3 times using the CT constrained and unconstrained Cobb methods based on the same set of rotated CT images (19 images with orientation interval of 5°) using the same protocol.

Statistical analyses

Statistical analyses were performed in SPSS (version 21, IBM, USA) with a significant level set at 0.05. The inter- and intra-reliability of PMC measurements obtained from the CM was evaluated using the intra-class correlation coefficient (ICC) with a two-way random model and absolute agreement with a 95% confidence interval. One-way repeated measures ANOVA was used to compare the difference between the repeated PMC obtained from the CM. The strength of reliability was evaluated using the criteria: very reliable (ICC: 0.8-1.0), moderately reliable (ICC: 0.60-0.79) and questionably reliable (ICC: <0.60) [12]. The validity of the PMC acquired using the CM was analysed according to the ICC, Bland-Altman method, and inter-method difference which included mean difference (MD), standard deviation (SD) and standard error mean (SEM). The linear regression analysis was also performed with the correlation coefficient: 0.75-1.00 indicating very good to excellent, 0.50-0.75 indicating moderate to good and 0.25-0.50 indicating poor correlation [13].

Results

A total of 52 curves were analysed in this study, including 28 RTs (mean coronal-Cobb: 46.8°±11.9° with a range of 26.2°-71.1°) and 24 LLs (mean coronal-Cobb: 30.9°±11.4° with a range of 16.4°-54.2°).

Mean trend of Cobb angle in different images of the spine

The mean trends of Cobb angle obtained using the CM as well as the CT constrained and unconstrained Cobb methods were similar in the RTs and LLs groups (Fig. 4). In comparison with the CM and constrained Cobb method, the unconstrained method offered a slightly larger mean Cobb angle in the LLs group.

Reliability assessment of the PMC estimation using the CM

As shown in Table 1, the intra-rater ICC values of PMC (PMC-Cobb & PMC-orientation) obtained using the CM were from 0.91 to 0.98 with no significant intra-rater difference ($p>0.05$) in the RTs and LLs groups. Moreover, the inter-rater ICC values varied from 0.84 to 0.92 and the inter-rater difference was not significant ($p>0.05$) (Table 2). Besides,

the intra- and inter-rater ICC values of the PMC acquired using the CM were similar to those of the coronal-Cobb (Tables 1 & 2).

Table 1. Intra-rater reliability of PMC estimation using the CM

PMC	Rater 1		Rater 2		Coronal	Rater 1		Rater 2	
Parameter	ICC	Sign.p	ICC	Sign.p	Parameter	ICC	Sign.p	ICC	Sign.p
RTs									
PMC-Cobb	0.951	0.196	0.983	0.059	Coronal-Cobb	0.956	0.135	0.982	0.205
PMC-orientation	0.913	0.171	0.949	0.051	-	-	-	-	-
LLs									
PMC-Cobb	0.971	0.065	0.977	0.970	Coronal-Cobb	0.971	0.064	0.985	0.055
PMC-orientation	0.958	0.473	0.982	0.112	-	-	-	-	-

Sign.p: significant level, p obtained from one-way repeated measures ANOVA
ICC: intra-class correlation coefficient

Table 2. Inter-rater reliability of the PMC estimation using the CM

PMC Parameter	Sign.p	ICC	Coronal Parameter	Sign.p	ICC
RTs					
PMC-Cobb	0.387	0.915	Coronal-Cobb	0.591	0.860
PMC-orientation	0.057	0.912	-	-	-
LLs					
PMC-Cobb	0.146	0.877	Coronal-Cobb	0.053	0.959
PMC-orientation	0.055	0.838	-	-	-

Sign.p: significant level, p obtained from paired t-test
ICC: intra-class correlation coefficient

Validity of PMC estimation using the CM

As shown in Table 3, high ICC values (0.91-0.97) were found between the PMC (PMC-Cobb & PMC-orientation) obtained using the CM, constrained and unconstrained Cobb methods for both the RTs and LLs groups. According to the Bland-Altman method assessment (Fig. 5), all the PMC of the CM and two Cobb methods almost distributed around the central lines, and the inter-method differences were small (RTs group: MD≤2.8° & ≤3.1°; LLs group: MD≤4.8° & 4.3°) (Table 3).

According to the linear regression analysis (Table 4), good to very good linear correlations were observed between the PMC acquired using the CM, constrained and unconstrained Cobb methods with a coefficient of determination R^2 of 0.69-0.89 and of 0.77-0.85 in the RTs and LLs groups, respectively. The generated linear regression equations could

be used to convert the PMC (x) of the CM to the corresponding PMC (y) of the constrained and unconstrained Cobb methods.

Time consumption in PMC estimation using the CM and CT Cobb methods

For the CM, average 5 and 8 minutes were required for manual identification of the eight corner points and all the procedures for the PMC calculation in Excel software for each curve, respectively, while an average of 20 minutes was needed when using the constrained or unconstrained Cobb method.

Table 3. Mean of and difference between the PMC obtained using the three methods

PMC Parameter	Mean PMC (mean ± SD) (°)			CM vs. Constrained Cobb Method				CM vs. Unconstrained Cobb Method			
	CM	Constrained Cobb method	Unconstrained Cobb method	Difference (°)			ICC	Difference (°)			ICC
				MD	SD	SEM		MD	SD	SEM	
RTs											
PMC-Cobb	48.3±11.4	50.4±12.7	51.1±12.9	2.5	4.2	0.8	0.968	2.8	4.3	0.8	0.966
PMC-orientation	-74.8±9.1	-73.4±8.9	-71.7±9.9	1.4	5.2	1.0	0.910	3.1	5.6	1.1	0.905
LLs											
PMC-Cobb	39.8±9.9	44.6±9.4	44.6±9.7	4.7	4.3	0.9	0.952	4.8	4.9	1.0	0.934
PMC-orientation	-234.8±16.3	-232.4±17.1	-230.5±16.9	2.4	6.7	1.4	0.958	4.3	7.1	1.5	0.952

MD: mean different, SD: standard deviation, Difference = constrained/unconstrained Cobb method - CM
SEM: standard error mean, ICC: intra-class correlation coefficient

Table 4. Linear regression analysis for the PMC estimation using the CM, constrained and unconstrained Cobb methods

PMC Parameter	CM (x) to Constrained Cobb Method (y)		CM (x) to Unconstrained Cobb Method (y)	
	Linear regression equation (°)	Coefficient of determination (R^2)	Linear regression equation (°)	Coefficient of determination (R^2)
RTs				
PMC-Cobb	y = 1.051x + 0.223	0.890	y = 1.052x + 0.330	0.892
PMC-orientation	y = 0.815x – 11.804	0.695	y = 0.876x – 6.168	0.685
LLs				
PMC-Cobb	y = 0.859x + 10.378	0.824	y = 0.864x + 10.561	0.766
PMC-orientation	y = 0.982x – 2.071	0.848	y = 0.953x – 6.473	0.826

Discussion

This study developed a purpose-design CM for the PMC (PMC-Cobb & PMC-orientation) estimation and verified the results with those data acquired from CT. The major findings included: (1) high intra- and inter-rater reliability of the PMC obtained using the CM was observed in the RTs and LLs groups; (2) good agreement and high correlation were found between the PMC of the CM, constrained and unconstrained Cobb methods in the RTs and LLs groups.

The PMC taken from the CM showed high intra- and inter-rater reliability for both the RTs and LLs (intra-ICC>0.9 & inter-ICC>0.8), which was similar to the strength of reliability of the coronal-Cobb measurements reported in this study as well as in the previous studies [14,15]. Besides, no significant intra- and inter-rater difference was found ($p>0.05$), indicating that the CM could provide reliable PMC for the RTs and LLs in this study.

A strong correlation was found between the PMC (PMC-Cobb & PMC-orientation) obtained using the CM, constrained and unconstrained Cobb methods (inter-method ICC>0.9). The assessments of the Bland-Altman method showed good agreement between the PMC of the CM and the two Cobb methods. Moreover, the inter-method mean difference (RTs group: MD≤2.8º & ≤3.1º; LLs group: MD≤4.8° & 4.3°) was within the clinically accepted threshold (5°) [16]. The SD values of the inter-method mean difference were not small in comparison with the inter-method mean difference itself (Table 3), and the zones of the Bland-Altman plots (Fig. 5) were slightly wide. This may be due to some outliers, in which greater variations of limits (the upper- and lower-end vertebrae) selected for the curvature measurements in the CM and two Cobb methods were observed as compared to those distributed closer to the center lines of the Bland-Altman plots. From this point, to improve the consistency of limits selection for curvature measurements between the CM and the two Cobb methods would reduce the inter-method difference of the PMC. Future study is needed to further evaluate and improve the validity of the CM in PMC estimation. Nonetheless, these results proved the validity of the CM in the PMC estimation. Besides, the generated regression equations could be used to convert the PMC obtained using the CM to the corresponding PMC acquired using the two Cobb methods for the RTs and LLs involved in this study ($R^2 \geq 0.7$).

The PMC has been used in the 3D assessment [8,17,18] and classification [19,20] of AIS as well as 3D correction evaluation of surgical [21,22] and orthotic [23,24] treatment. Since providing information for the “true” magnitude of spinal curvature and the degree of spinal curve segment being rotated towards the coronal plane, the PMC may be superior to other clinical indices, such as the coronal-Cobb and axial vertebral rotation, in describing the 3D features of AIS. As reported by Labelle H et al. [6], a curve type classified by the Lenke system could be further split into different sub-types based on the PMC. Different curve sub-types may require different orthotic or surgical strategies. Thus, it may be necessary to employ the PMC as a supplement to the coronal-Cobb in clinical assessment and management of scoliosis.

Since the CM is merely based on the coronal and sagittal images of the spine, it can be applied to estimate the PMC of scoliosis from X-ray or EOS images (with both coronal & sagittal images). The first stage development of this purpose-design CM relied on the 3rd party software and it will be further developed under a new software with a user-friendly

operation interface. It will require less than 5 minutes to estimate the PMC, remarkably reducing the time-consuming issue. With the enhanced features, the CM could have a better potential to serve the 3D assessment of AIS.

There are some limitations to this study. The results presented in this study were based on the prone CT images of the subjects with wide age and curve ranges (age: 10-30; prone coronal-Cobb: 16° to 71°). The curves were grouped according to different types (RTs and LLs) while the factor of curve severity was ignored. Besides, this was not a large-sample study. For better understanding the properties (reliability and validity) of this developed CM, future study should be conducted with different curve severities (such as coronal-Cobb at 20°-40°, 40°-60° and 60°-80°) on more subjects.

Conclusion

A purpose-design computational method for the PMC estimation of scoliosis has been developed and the results showed that this method could provide reliable and valid PMC for the subjects with AIS. The findings of this study suggested that this computational method may have the potential to serve 3D assessment of AIS.

Captions

Fig.1 Plane of maximum curvature (PMC)

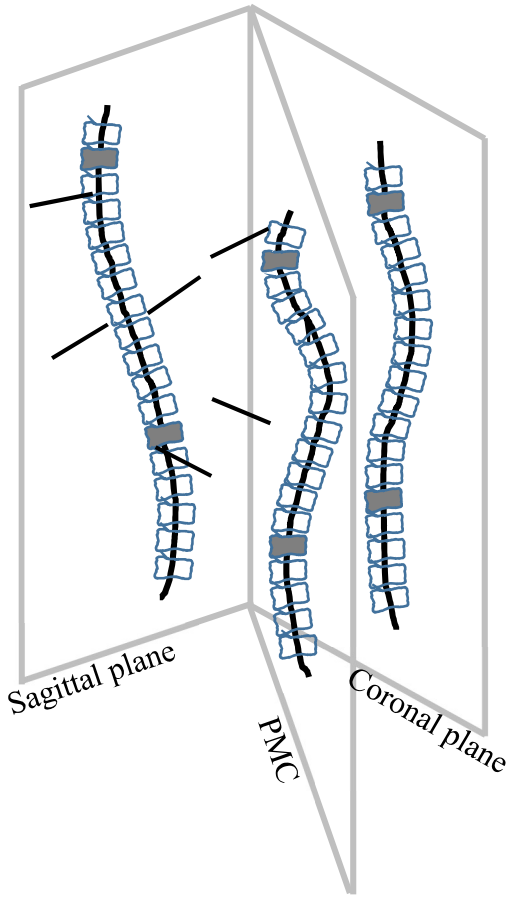

Fig.2 The superior endplate of the upper-end vertebra and inferior endplate of the lower-end vertebra of a specific spinal curve are assumed to be on the planes that can be extended outward named $Plane_{superior\text{-}endplate}$ and $Plane_{inferior\text{-}endplate}$, respectively. A vertical plane intersects with $Plane_{superior\text{-}endplate}$ and $Plane_{inferior\text{-}endplate}$ at $L_{vertical\text{-}superior}$ and $L_{vertical\text{-}inferior}$, respectively; and the angle (β) formed by the intersection lines is the Cobb angle of the spinal curve in that vertical plane

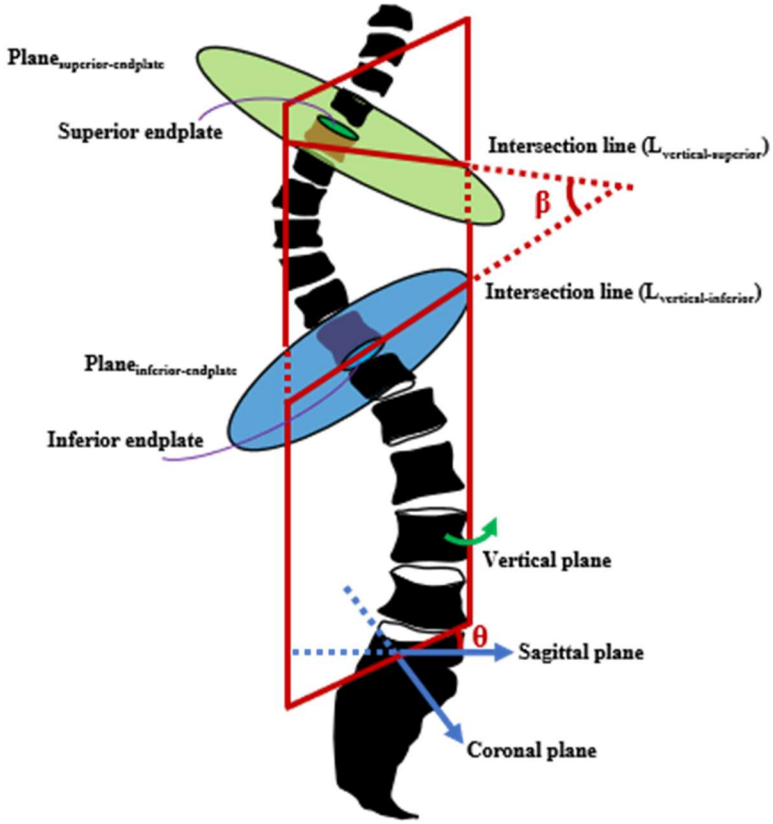

Fig. 3 The process of the PMC estimation for a specific case: a) The CM: a rater identified the eight corner points of the superior endplate of the upper-end vertebra and the inferior endplate of the lower-end vertebra in the sagittal and coronal images of the spine respectively, and the 3D coordinates of the eight corner points were used to calculate the Cobb angles in different planes with orientation interval of 1º. The maximum Cobb angle could be then determined, and the plane with the maximum Cobb angle would be PMC; & b) The constrained and unconstrained Cobb methods: Cobb angles in different projected images of the spine with orientation interval of 5º were measured using the constrained (solid lines) and unconstrained (dashed lines, italic) Cobb methods. The maximum Cobb angle of each method was identified, and the corresponding PMC was then determined. The PMC measurements of the CM and constrained and unconstrained Cobb methods were compared for validation purpose

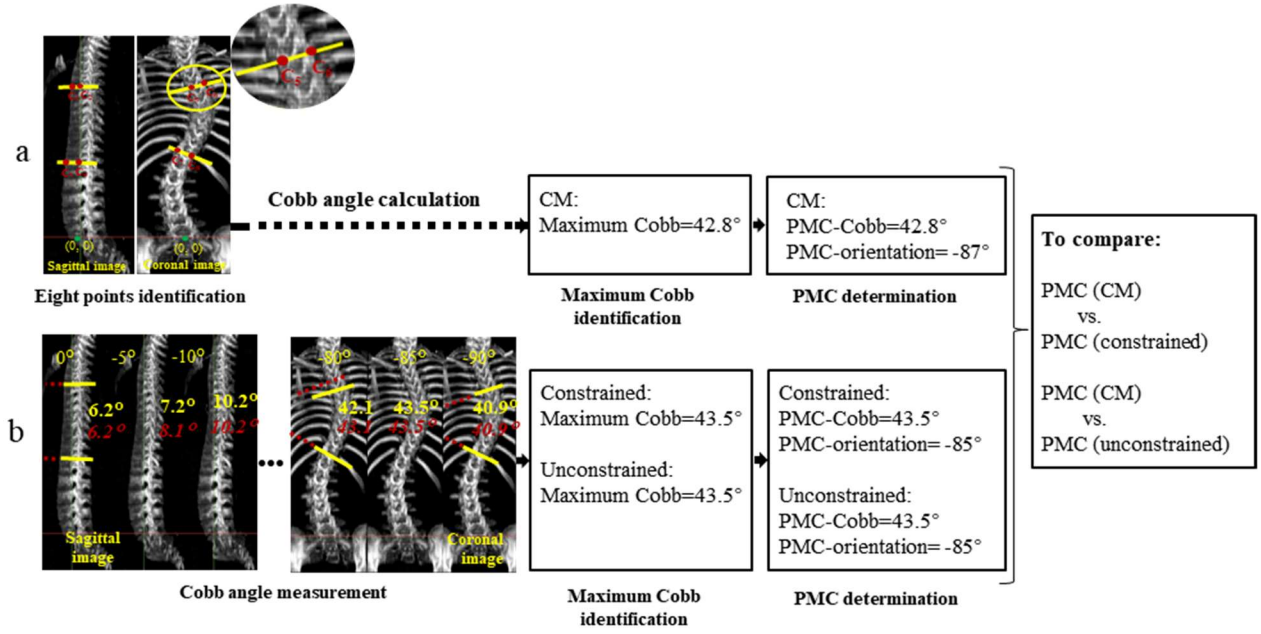

Fig. 4 The mean Cobb angles obtained using the three methods in different images of the spine in the RTs and LLs groups. From the top view, the x-axis/y-axis pointing to the posterior/right side represents the sagittal plane (orientation = 0°)/the coronal plane (orientation = -90°), respectively. The distance from the origin to each circle represents the magnitude of Cobb angle

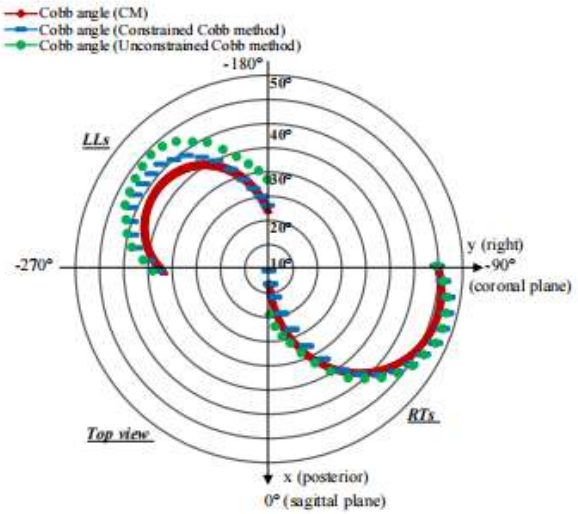

Fig.5 The Bland-Altman plot assessing the agreement of the PMC obtained using the CM, constrained and unconstrained Cobb methods in the RTs and LLs groups (mean = (constrained/unconstrained Cobb method + CM)/2; difference = constrained/unconstrained Cobb method - CM)

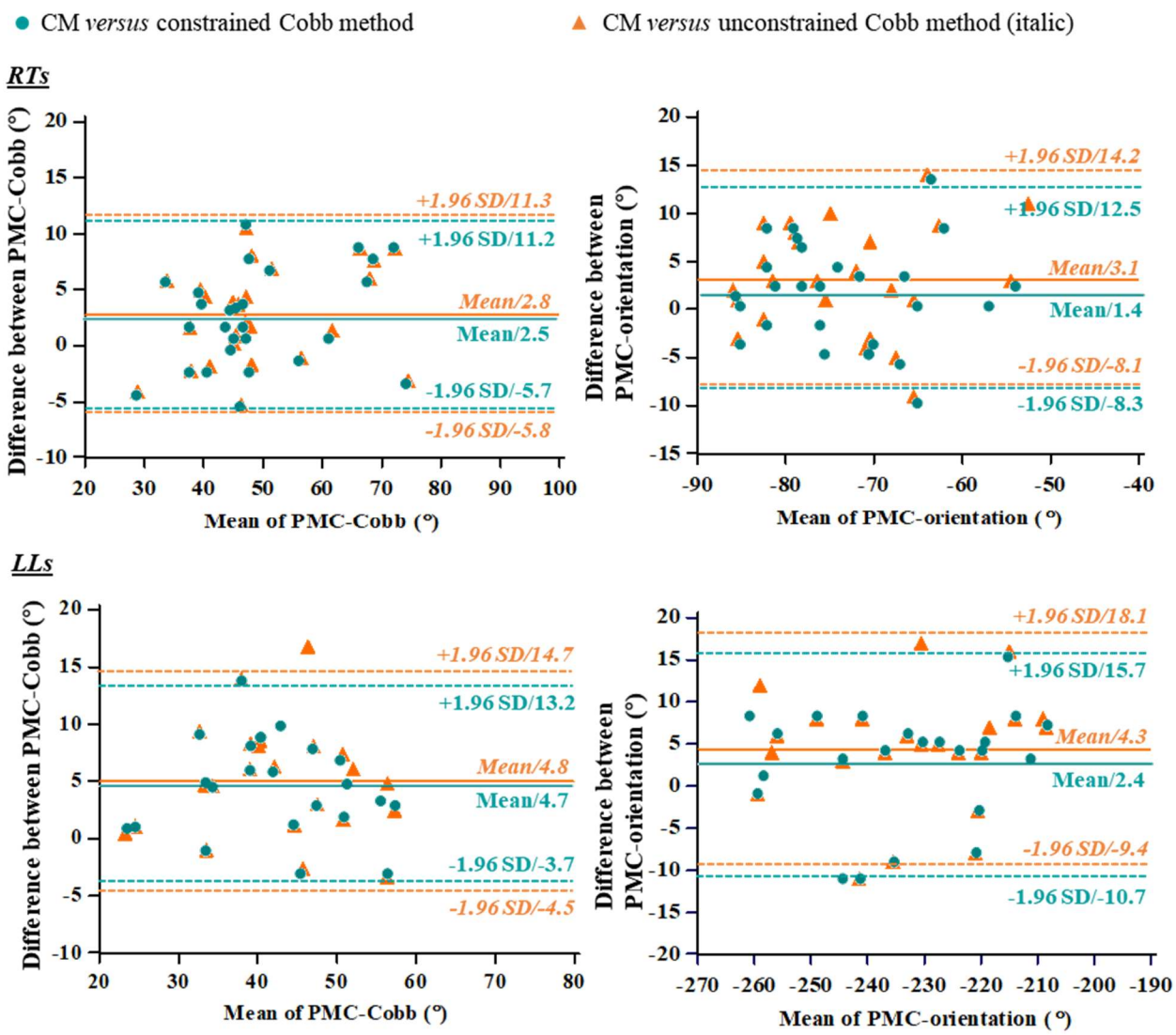

References

1. Stokes IAF (1994) Three-dimensional terminology of spinal deformity: a report presented to the scoliosis research society by the Scoliosis Research Society working group on 3-D terminology of spinal deformity. Spine 19:236-248
2. Kotwicki T, Negrini S, Grivas TB, Rigo M, Maruyama T, Durmala J, Zaina F (2009) Methodology of evaluation of morphology of the spine and the trunk in idiopathic scoliosis and other spinal deformities - 6th SOSORT consensus paper. Scoliosis 4:1-16
3. Villemure I, Aubin CE, Grimard G, Dansereau J, Labelle H (2001) Progression of vertebral and spinal three-dimensional deformities in adolescent idiopathic scoliosis: a longitudinal study. Spine 26:2244-2250
4. Sangole AP, Aubin CE, Labelle H, Stokes IAF, Lenke LG, Jackson R, Newton P (2008) Three-dimensional classification of thoracic scoliotic curves. Spine 34:91-99
5. Aubin CE, Lobeau D, Labelle H, Maquinghen-Godillon AP, LeBlanc R, Dansereau J (1999) Planes of maximum deformity in the scoliotic spine. In: IAF Stokes (ed) Research into spinal deformities 2, IOS Press, Amsterdam, pp 45-48
6. Labelle H, Aubin CE, Jackson R, Lenke L, Newton P, Parent S (2011) Seeing the spine in 3D: how will it change what we do? J Pediatr Orthop 31:S37–S45
7. Lenke LG (2012) What's new in the surgical care of adolescent idiopathic scoliosis (AIS). Argo Spine News & Journal 24:62-66
8. Stokes IAF, Bigalow LC, Moreland MS (1987) Three-dimensional spinal curvature in idiopathic scoliosis. J orthop Res 5:102-113
9. Trac S, Zheng R, Hill DL, Lou E (2019) Intra- and interrater reliability of Cobb angle measurements on the plane of maximum curvature using ultrasound imaging method. Spine Deform 7:18-26
10. Sangole A, Aubin CE, Labelle H, Lenke L, Jackson R, Newton P, Stokes IAF (2010) The central hip vertical axis: a reference axis for the three-dimensional classification of idiopathic scoliosis. Spine 35:E530-534
11. Koreska J, Smith JM (1982) Portable desktop computer-aided digitiser system for the analysis of spinal deformities. Med & Biol Eng Compu 20:715-726
12. Currier DP (1984) Elements of research in physical therapy. 3rd edn. William & Wikins, Baltimore.
13. Dawson B, Trapp RG (2004) Basic and clinical biostatistics. 4th edn. Lange Medical Books/McGraw-Hill, New York
14. Hong JY, Suh SW, Modi HN, Hur CY, Song HR, Ryu JH (2011) Centroid method: reliable method to determine the coronal curvature of scoliosis: a case control study comparing with the Cobb method. Spine 36:E855-E861
15. Tanure MC, Pinheiro AP, Oliveira AS (2010) Reliability assessment of Cobb angle measurements using manual and digital methods. Spine J 10:769-774
16. Wu H, Ronsky JL, Cheriet F, Harder J, Kupper JC, Zernicke RF (2011) Time series spinal radiographs as prognostic factors for scoliosis and progression of spinal deformities. Eur Spine J 20:112-117
17. Stokes IAF (1989) Axial rotation component of thoracic scoliosis. J orthop Res 7:702-708

18. Nault ML, Mac-Thiong JM, Roy-Beaudry M, Turgeon I, Deguise J, Labelle H, Parent S (2014) Three-dimensional spinal morphology can differentiate between progressive and nonprogressive patients with adolescent idiopathic scoliosis at the initial presentation: a prospective study. Spine 39:E601-606
19. Kadoury S, Labelle H (2012) Classification of three-dimensional thoracic deformities in adolescent idiopathic scoliosis from a multivariate analysis. Eur Spine J 21:40-49
20. Duong L, Mac-Thiong JM, Cheriet F, Labelle H (2009) Three-dimensional subclassification of Lenke type 1 scoliotic curves. J Spinal Disord Tech 22:135-143
21. Labelle H, Dansereau J, Bellefleur C, Poitras B, Rivard CH, Stokes IA, de-Guise J (1995) Comparison between preoperative and postoperative three-dimensional reconstructions of idiopathic scoliosis with the Cotrel-dubousset procedure. Spine 20:2487-2492
22. Delorme S, Labelle H, Aubin CE, Guise JAd, Rivard CH, Poitras B, Dansereau J (2000) A three-dimensional radiographic comparison of Cotrel–Dubousset and Colorado instrumentations for the correction of idiopathic scoliosis. Spine 25:205-210
23. Labelle H, Dansereau J, Bellefleur C, Poitras B (1996) Three-dimensional effect of the Boston brace on the thoracic spine and rib cage. Spine 21:59-64
24. Labelle H, Bellefleur C, Joncas J, Aubin CE, Cheriet F (2007) Preliminary evaluation of a computer-assisted tool for the design and adjustment of braces in idiopathic scoliosis: a prospective and randomized study. Spine 32:835-884